This is a preprint, the final version is subject to change, of the American Mineralogist (MSA)
Cite as Authors (Year) Title. American Mineralogist, in press.
(DOI will not work until issue is live.) DOI: http://dx.doi.org/10.2138/am-2015-5117

Revision 1

Pieczkaite, ideally $Mn_5(PO_4)_3Cl$, a new apatite-supergroup mineral from Cross Lake, Manitoba, Canada: Description and crystal structure

Kimberly Tait[1,2], Neil A. Ball[1] and Frank C. Hawthorne[1,*]

[1] Department of Geological Sciences, University of Manitoba,
Winnipeg, Manitoba, R3T 2N2, Canada

[2] Current address: Department of Natural History (Mineralogy), Royal Ontario Museum,
100 Queen's Park, Toronto, Ontario, M5S 2C6, Canada

* E-mail: frank_hawthorne@umanitoba.ca

ABSTRACT

Pieczkaite, ideally $Mn_5(PO_4)_3Cl$, is a new apatite-supergroup mineral from Cross Lake, Manitoba, Canada. It occurs as small patches and narrow veins in large crystals of apatite and (Mn,Cl)-bearing apatite in phosphate pods in the quartz core of a granitic pegmatite. Veins of Mn-bearing apatite narrow to ~25 microns where the Mn content becomes high enough to constitute pieczkaite. It is grey with a greyish-white streak, does not fluoresce under ultraviolet light, and has no observable cleavage or parting. Mohs hardness is 4–5, and pieczkaite is brittle with an irregular fracture. The calculated density is 3.783 g/cm^3. Optical properties were measured using a Bloss spindle stage at a wavelength of 590 nm (using a gel filter). Pieczkaite is uniaxial (–) with indices of refraction $\omega = 1.696$, $\varepsilon = 1.692$, both ±0.002. Pieczkaite is hexagonal, space group $P6_3/m$, a 9.504(4), c 6.347(3) Å, V 496.5(1) Å^3, Z = 2, c:a = 1:0.6678. The six strongest lines in the X-ray powder diffraction pattern are as follows: d (Å), I, (h k l): [note to typesetting: changes minus signs to overbars] 2.794, 100, (-2 3 1, -1 3 1); 2.744, 88, (0 3 0); 2.639, 34, (-1 2 2); 2.514, 25, (0 3 1, 0 2 2); 1.853, 25, (-3 4 2, -1 4 2); 3.174, 24, (0 0 2). Chemical analysis by electron microprobe gave P_2O_5 37.52, MnO 41.77, FeO 2.45, CaO 13.78, Cl 3.86, H_2O 0.60, O ≡ Cl –0.87, sum 99.11 wt.% where the H_2O content was calculated as 1 – Cl apfu. The resulting empirical formula on the basis of 12 O anions is $(Mn_{3.36}Fe_{0.20}Ca_{1.40})_{\Sigma 4.96}$ $(P_{1.01}O_4)_3(Cl_{0.62}OH_{0.38})_{1.00}$, and the end-member formula is $Mn_5(PO_4)_3Cl$. The crystal structure of pieczkaite was refined to an R_1 index of 4.07% based on 308 observed reflections collected on a three-circle rotating-anode diffractometer with Mo$K\alpha$ X-radiation. Pieczkaite is isostructural with apatite, Mn is the dominant cation at both the [9]- and [7]-coordinated-cation sites in the structure, and Cl is the dominant monovalent anion.

Keywords: Pieczkaite, new mineral species, phosphate, apatite supergroup, granitic pegmatite, Cross Lake, Manitoba, Canada, crystal structure, electron-microprobe analysis, Raman spectrum.

INTRODUCTION

Pegmatite #22 occurs on the southeastern shoreline of a small, unnamed island in Cross Lake, Manitoba, Canada. It was investigated as part of general work on the Cross Lake Pegmatite field (Anderson 1984), and a very Mn-rich assemblage of phosphate minerals was discovered. Bobfergusonite (Ercit et al. 1986a, 1986b) was discovered in samples collected at this time, together with an unknown phosphate whose structure remained somewhat enigmatic for many years. More recently, Tait (2002) examined the mineralogy of the phosphate nodules in pegmatite #22 in considerable detail, and Ercit et al. (2010) and Tait et al. (2011) described the hitherto unknown phosphate mineral as manitobaite, an ordered superstructure of the alluaudite structure type. The nodules contained large crystals of Mn-rich apatite, and a Mn-dominant apatite-like phase occurred in fractures in these crystals. This material was characterized as a (Mn,Cl)-dominant analogue of apatite. The new mineral and mineral name were approved by the Commission on New Minerals and Mineral Names, International Mineralogical Association (IMA 2014-005). Pieczkaite is named after Adam Pieczka (born 1957-09-08 at Wilamowice near Bielsko-Biała, Silesia Province, Poland), Assistant Professor in the Department of Mineralogy, Petrography and Geochemistry, Faculty of Geology, Geophysics and Environmental Protection, Kraków, Poland, for his extensive contributions to the crystal chemistry of pegmatite minerals. The holotype is deposited in the mineral collection of the Royal Ontario Museum, catalogue number M56483.

SAMPLE PROVENANCE

Pieczkaite occurs in pegmatite #22 on the southeastern shoreline of a small, unnamed island in Cross Lake, Manitoba, Canada, about 5 km north-northwest of the Cross Lake

settlement at 54°41′N 97°49′W (Anderson 1984; Ercit et al. 1986a, 1986b). Associated minerals in the interior wall zone of the pegmatite are fluorapatite, bobfergusonite, manitobaite, eosphorite, dickinsonite, triploidite, goyazite, perloffite, beusite, triplite, quartz, K-feldspar, muscovite, schorl, beryl, spessartine, gahnite and (Nb,Ta, Sn)-oxides. In the core zone, the associated minerals are fluorapatite, chlorapatite, triploidite, eosphorite, dickinsonite, fillowite, quartz, K-feldspar, muscovite, schorl, beryl, gahnite and (Nb,Ta,Sn)-oxides. Fluorapatite is a common primary mineral in the core zone of the pegmatite, whereas Mn-rich Cl-rich apatite and pieczkaite occur in the interior wall zone as narrow veins and small inclusions in apatite and fine-grained aggregates of manitobaite, eosphorite, triploidite, etc., indicating crystallization from late-stage, residual pegmatitic fluids highly enriched in Mn and Cl.

PHYSICAL PROPERTIES

Pieczkaite occurs as patches and veins in large crystals of apatite and Mn-bearing apatite in phosphate pods in the quartz core of a granitic pegmatite. The Mn content is inversely proportional to the size of the patches and the width of the veins. Continuous veins consist of Mn-bearing apatite, narrowing to ~25 microns where the Mn content becomes high enough to constitute pieczkaite. It is grey with a greyish-white streak, does not fluoresce under ultraviolet light, and has no observable cleavage or parting. Mohs hardness is 4–5, and pieczkaite is brittle with an irregular fracture. The calculated density is 3.783 g/cm^3. Optical properties were measured using a Bloss spindle stage at a wavelength of 590 nm (using a gel filter). Pieczkaite is uniaxial (–) with indices of refraction $\omega = 1.696$, $\varepsilon = 1.692$, both ±0.002.

CHEMICAL COMPOSITION

Crystals were analyzed with a Cameca SX-100 electron microprobe operating in wavelength-dispersion mode with an accelerating voltage of 15 kV, a specimen current of 10 nA, and a beam diameter of 5 μm. The following standards were used: maricite (P, Fe), spessartine (Mn), apatite (Ca), tugtupite (Cl). The data were reduced and corrected by the *PAP* method of Pouchou and Pichoir (1985). Table 1 gives the chemical composition (mean of seven determinations). The empirical formula unit, based on 12 O atoms per formula unit (pfu) with (Cl + OH) = 1 apfu, is $(Mn_{3.36}Fe_{0.20}Ca_{1.40})_{\Sigma 4.96}(P_{1.01}O_4)_3(Cl_{0.62}OH_{0.38})_{1.00}$, the general formula is $(Mn, Ca)_5(PO_4)_3(Cl,OH)$ and the end-member formula is $Mn_5(PO_4)_3Cl$.

X-RAY POWDER DIFFRACTION

The nature of the sample did not provide sufficient material of the composition of pieczkaite to allow collection of powder diffraction data. Thus we collapsed the single-crystal data to produce an experimental diffraction pattern that simulates that of a powder pattern, in much the same way that a Gandolfi apparatus does. The resulting data are listed in Table 2.

RAMAN AND INFRARED SPECTROSCOPY

The Raman spectrum was collected in back-scattered mode on a HORIBA Jobin Yvon-LabRAM ARAMIS integrated confocal micro-Raman system equipped with a 460 mm focal length spectrograph and a multichannel air-cooled (–70°C) CCD detector. A magnification of 1006 was used with an estimated spot size of 1 mm, an 1800 lines mm^{-1} grating, an excitation radiation of 532 nm, and a laser power between 5 and 12.5 mW. The spectrometer was calibrated using the 520.7 cm^{-1} line of silicon. The Raman spectrum is shown in Figure 1a. The peaks at

~1095 cm^{-1} (strong), ~1000 and 960 cm^{-1} (shoulders) may be assigned to stretching vibrations of the PO_4 groups, and the peak at ~795 cm^{-1} (weak) to HPO_4 stretches. The peak at 560 and shoulder at ~480 cm^{-1} are due to bending vibrations of PO_4. In the infrared (Fig. 1b), the OH band is centered at ~3460 cm^{-1} and has significant fine structure due to different local arrangements of Mn and Ca bonded to (OH).

The Fourier transform infrared (FTIR) spectrum was collected using a Bruker Hyperion 2000 IR microscope equipped with a liquid-nitrogen-cooled mercury-cadmium-telluride detector. The spectrum was obtained in the range 4000-650 cm^{-1} by averaging 100 scans with a resolution of 4 cm^{-1}. A very broad envelope centred at ~3450 cm^{-1} (Fig. 1b) and the lack of peaks at ~1630 cm^{-1} are indicative of the presence of (OH) in pieczkaite.

CRYSTAL-STRUCTURE SOLUTION AND REFINEMENT

A single crystal of pieczkaite (8 x 25 x 30 μm) was attached to a glass fiber and mounted on a Bruker D8 three-circle diffractometer equipped with a rotating anode generator (MoKα X-radiation), multilayer optics and an APEX-II detector. A total of 11,949 intensities was measured out to 50° 2θ using 14 s per 0.5° frame with a crystal-to-detector distance of 5 cm. Unit-cell dimensions were determined by least-squares refinement of 4082 reflections with $I > 10\sigma I$, and are given in Table 3, together with other information pertaining to data collection and structure refinement. Empirical absorption corrections (SADABS; Sheldrick 2008) were applied and the data were corrected for Lorentz, polarization and background effects, averaged and reduced to structure factors, resulting in 325 unique reflections.

All calculations were done with the SHELXTL PC (Plus) system of programs; *R* indices are of the form given in Table 3 and are expressed as percentages. Systematic absences in the

single-crystal X-ray diffraction data are consistent with space group $P6_3/m$, and the structure was refined by full-matrix least-squares to an R_1 index of 4.07% using a fully ionized scattering factor for oxygen and neutral scattering factors for other species (see Lussier et al. 2011; Cooper et al. 2009; Abdu and Hawthorne 2013). Refined atom coordinates and anisotropic-displacement parameters are listed in Table 4, selected interatomic distances are given in Table 5, refined site-scattering values are listed in Table 6, and bond valences [calculated with the parameters of Brown (2013) and Brese and O'Keeffe (1991)] are given in Table 7.

CRYSTAL STRUCTURE

Pieczkaite has the apatite structure (e.g., Hughes et al. 1990; Hughes and Rakovan 2002). The refined site-scattering values (Hawthorne et al. 1995) given in Table 6 are compatible with the chemical formula calculated from the electron microprobe analysis, and show that the M1 and M2 sites are occupied by Mn and Ca. Mn is the dominant cation at both the M1 and M2 sites, and Cl is the dominant anion at the monovalent-anion X site, and hence the end-member composition of pieczkaite is $Mn_5(PO_4)_3Cl$.

Of particular interest in the structure of pieczkaite is the stereochemistry of the M1 and M2 sites, and their relation to the stereochemistry of the analogous sites in hydroxylapatite (Hughes et al. 1989), synthetic fluorapatite (Sudarsanan et al. 1972) and synthetic chlorapatite (Mackie et al. 1972). Hydroxylapatite, fluorapatite and pieczkaite are hexagonal and have space-group symmetry $P6_3/m$, whereas chlorapatite is monoclinic and has space-group symmetry $P2_1/b$ (first setting). The result of this lowering in symmetry is that in chlorapatite, there are two sites, Ca1 and Ca2, that are analogous to the M1 site in the $P6_3/m$ apatite structure, and three sites, Ca3, Ca4 and Ca5, that are analogous to the M2 site in the $P6_3/m$ apatite structure.

The stereochemistry of the M1, Ca1 and Ca2 sites in hydroxylapatite, fluorapatite, chlorapatite and pieczkaite is shown in Figure 2, and the M1-O and M2-O,X ($X = OH^-$, F^-, Cl^-) distances are compared in Table 8. The conformation of the coordination of the M1 site is very similar in all four structures (Fig. 2). The M1 site in pieczkaite has a smaller mean bond-length than the other three apatite structures (Table 8), in accord with the smaller cation radius of Mn^{2+} relative to that of Ca. Shannon (1976) gives $^{[9]}Ca^{2+} = 1.18$, $^{[3]}O^{2-} = 1.36$ Å, sum = 2.54 Å, close to the observed <M1-O> distance of 2.55 Å in hydroxylapatite and fluorapatite (Table 7). Comparison of <M1-O> bond-lengths in Table 8 shows that these distances in hydroxylapatite, fluorapatite and chlorapatite are very similar at ~2.55 Å, indicating that the presence of Cl^- at the X site has no inductive effect on the size of the M1 polyhedron in chlorapatite (even though it does cause a lowering of symmetry). This <M1-O> distance of ~2.55 Å is significantly longer (by ~0.08 A) than the analogous distance in pieczkaite: 2.473 Å (Table 8). Shannon (1976) does not list a radius for $^{[9]}Mn^{2+}$, but we may derive a value by extrapolation from his listed radius values for other coordination numbers of Mn^{2+}: $^{[9]}Mn^{2+} = 1.04$ Å. Summing the relevant values gives a predicted <M1-O> distance in pieczkaite of (1.04 x 1.15 + 1.18 x 0.85) / 2 + 1.375 ≈ 2.475 Å, close to the observed value of 2.47 Å (Table 8). Should the M1-O(3) distance be considered as a chemical bond where *M*(1) is occupied by Mn^{2+}? Inspection of the bond valences (Table 7) indicates that the incident bond-valence sums around O3 and, to a lesser extent, M1, are low if M1-O3 is not considered as a chemical bond. If the M1-O3 distance is considered as a bond in pieczkaite, the sum at the O3 anion becomes more reasonable (1.954 v.u., Table 7), but the sum at the M1 site is somewhat large (2.151 v.u.). All things considered, it seems that a coordination number of [9] is somewhat more appropriate for Mn^{2+} at the M1 site in pieczkaite, although the situation is not clearcut.

The coordination of the M2 site (and the analogous Ca3, Ca4 and Ca5 sites in chlorapatite) shows much more variation than at the M1 site (Fig. 3). In fluorapatite, the F atom occurs on the mirror plane at $z = 1/4$, whereas in hydroxylapatite and pieczkaite, the monovalent anion is displaced slightly off the mirror plane at $z = ¼$. In chlorapatite, the monovalent anion is further displaced off the mirror plane (Fig. 3c). In hydroxylapatite and pieczkaite, only one of the monovalent anions shown in Figure 3 can bond to the M2 cation, as the other site is too close to be occupied. The coordination of the monovalent anion in these four structures is shown in Figure 4. The X site in all structures is surrounded by six M2 cations at the vertices of an octahedron. In hydroxylapatite, fluorapatite and pieczkaite, the monovalent anion occurs close to a face of this octahedron (Figs. 4a, b, d) whereas in chlorapatite, the monovalent anion is displaced toward the centre of this octahedron (Fig. 4c). As a result of these arrangements, the monovalent anion in hydroxylapatite, fluorapatite, chlorapatite and pieczkaite is bonded to three M2 cations at distances in the range 2.23-2.80 Å. The relevant bond lengths and bond valences are listed in Table 9. Here we see the reason why the monovalent anion occupies different positions in fluorapatite, hydroxylapatite, chlorapatite and pieczkaite. In fluorapatite, F occurs exactly in the plane of the three coordinating Ca^{2+} cations as the resulting bond lengths provide sufficient incident bond-valence to F^- to satisfy the valence-sum rule of bond-valence theory. In hydroxylapatite, OH^- is slightly displaced from the plane of the three coordinating Ca^{2+} cations and has longer X-Ca distances (Table 9), and the corresponding Ca^{2+}-OH^- distances result in incident bond-valences that again are in accord with the valence-sum rule around OH^-. In chlorapatite, Cl^- is displaced significantly from the plane of the three coordinating Ca^{2+} cations (Fig. 4c) and has much longer X-Ca distances (Table 9), and the corresponding Ca^{2+}-Cl^- distances result in incident bond-valences that again are in accord with the valence-sum rule

around Cl^-. In pieczaite, the X anion (= $Cl^-_{0.62}OH^-_{0.38}$) is displaced only slightly from the plane of the three coordinating Mn^{2+} cations (Fig. 4c) and has much shorter X-Mn^{2+} distances that in chlorapatite (Table 9), and the corresponding Mn^{2+}-(Cl^-,OH^-) distances result in incident bond-valences that again are in accord with the valence-sum rule around Cl^-. Thus we see the reason why Cl occupies a very different position in the structure of pieczkaite than in the structure of chlorapatite: the occurrence of Mn^{2+} instead of Ca^{2+} at M2 requires the Cl^- anion to displace from its position intermediate between the face and the centre of the octahedron of surrounding M2 cations (in chlorapatite, Fig. 4c) almost to the plane of the edge of the octahedron (in pieczkaite, Fig. 4d) in order to satisfy its bond-valence requirements. The situation is much more complicated in minerals which show F^-, Cl^-, O^{2-} solid-solution as local order-disorder between the different anion species become important (Hughes et al. 1990; Hughes and Rakovan 2002).

ORDERING OF Mn^{2+} IN THE APATITE STRUCTURE

Long-range order

Several previous studies have shown that Mn^{2+} tends to order at the M1 site (Suitch et al. 1985; Hughes et al. 2004). This constrasts with the present results which show Mn^{2+} more strongly ordered at M2 [Mn^{2+} / (Mn^{2+} + Ca) = 0.82] than at M1 [Mn^{2+}/ (Mn^{2+} + Ca) = 0.575] in pieczkaite. Inspection of the chemical formulae of the relevant structures shows that where Mn^{2+} tends to order at the M1 site, the X site is occupied by F, whereas in pieczkaite, the X site is occupied by Cl. It is apparent that the nature of the monovalent anion strongly affects the ordering of Mn^{2+} in the apatite structure.

Short-range order

All cations at the M2 site in pieczkaite occupy approximately the same position at z = 0.2179 (Table 4). There is no sign of any residual electron density corresponding to the Cl position in chlorapatite, i.e., much nearer to the centre of the octahedra of M2 cations, as would be the case if Ca were bonded to Cl^-. This means that all Ca must be locally associated with OH^- at the neighboring X sites. There is 0.28 OH^- occupying the X site in pieczkaite (Table 6) and this must be locally associated with 0.28 x 3 = 0.84 apfu of M2 cations. As all Ca must be bonded to OH-, this means that the 0.28 OH- is bonded to 0.54 Ca + 0.30 Mn^{2+}, and all Cl is bonded to Mn^{2+}. The fine structure in the infrared spectrum in the principal OH-stretching region in pieczkaite must result from various local combinations of Ca and Mn^{2+} that sum to 0.54 Ca + 0.30 Mn^{2+} apfu: OH-CaCaCa, OH-CaCaMn^{2+}, OH-Ca$Mn^{2+}Mn^{2+}$ and OH-$Mn^{2+}Mn^{2+}Mn^{2+}$ in order of decreasing wavenumber as coordinating ions of greater mass shift the associated OH absorption to lower energies. If the arrangements OH-CaCaCa, OH-CaCaMn^{2+}, OH-Ca$Mn^{2+}Mn^{2+}$ and OH-$Mn^{2+}Mn^{2+}Mn^{2+}$ are random, they will occur in the following ratios: 0.49:0.27 : 0.15:0.08. Inspection of Figure 1b shows that this is not the case. The arrangement OH-CaCaCa must correspond to the highest-energy absorption which is at ~3596 cm^{-1}. This is fairly close to the value of 3570 cm^{-1} for hydroxylapatite, and the slightly higher value in pieczkaite may be due to Mn^{2+} at next-nearest-neighbor M sites. The relative intensity of this band (Fig. 1b) is significantly less than at least two of the lower-energy bands, indicating that there is strong short-range order of Ca and Mn^{2+} at these M2 trimers. Unfortunately we cannot use the relative band intensities to derive the amounts of these different short-range arrangements as we do not know the relation between transition probability and energy for the arrangements in

this structure type. Suffice it to say that strong short-range order of Ca and Mn^{2+} is indicated at M2 sites around the X site.

IMPLICATIONS

In the recently published IMA nomenclature of the apatite supergroup (Pasero et al. 2010), a Mn-rich apatite described by Pieczka (2007) is tentatively assigned to the hedyphane group on the assumption that Mn^{2+} is ordered at the M1 site and the end-member formula is $Mn^{2+}_2Ca_3(PO_4)_3Cl$. However, Mn^{2+} is more strongly ordered at M2 where X = Cl, and a more appropriate end member composition is $Ca_2Mn^{2+}_3(PO_4)_3Cl$ for compositions where Mn^{2+} is dominant at M2 and Ca is dominant at M1. However, the results of Suitch et al. (1985) and Hughes et al. (2004) show that Mn^{2+} is more strongly ordered at M1 where X = F, and a hedyphane-like end-member composition of $Mn^{2+}_2Ca_3(PO_4)_3F$ seems likely for F-rich compositions. However, extreme fractionation at late stages in pegmatite evolution produce residual fluids that react with earlier-crystallized minerals to produce common structures highly enriched in such elements as Mn, Pb and Cl. The stoichiometry of pieczkaite, $Mn^{2+}_5(PO_4)_3Cl$ show it to be an apatite-group mineral, the Mn^{2+} analogue of chlorapatite, pyromorphite and alforsite. It is very interesting that pyromorphite and alforsite have much larger M cations (Pb^{2+}, Ba) than apatite (Ca) whereas pieczkaite has a much smaller M cation (Mn^{2+}) than apatite (Ca). The placement of the Cl^- in pieczkaite is very similar to the placement of F^- in fluorapatite and $(OH)^-$ in apatite. $Mn_5(PO_4)Cl$ with the apatite structure was synthesized by Kreidel and Hummel (1970) at 850°C, whereas Yoder et al. (2004) were unable to synthesize $Mn_5(PO_4)Cl$ with the apatite structure from aqueous solution at a range of pH and temperatures (5-80°C). This result is in accord with the paragenesis of pieczkaite which suggests that the presence of Mn and Cl in

pieczkaite associated with F,Mn-rich apatite may be the result of enrichment of Mn-Cl complexes in late-stage fluids.

ACKNOWLEDGEMENTS

We thank John Hughes and Claude Yoder for their salient comments on this paper, and Mark Cooper for his help with this work. Supported was provided by a Canada Research Chair in Crystallography and Mineralogy and by Discovery and Major Installation grants from the Natural Sciences and Engineering Research Council of Canada to FCH, and by Innovation Grants from the Canada Foundation for Innovation to FCH.

REFERENCES

Abdu, Y.A., and Hawthorne, F.C. (2013) Local structure in *C2/c* clinopyroxenes on the hedenbergite ($CaFeSi_2O_6$)-ferrosilite ($Fe_2Si_2O_6$) join: A new interpretation for the Mössbauer spectra of Ca-rich *C2/c* clinopyroxenes and implications for pyroxene exsolution. American Mineralogist, 98, 1227–1234.

Anderson, A.J. (1984) The Geochemistry, Mineralogy and Petrology of the Cross Lake Pegmatite Field, Central Manitoba. MSc thesis, University of Manitoba, Winnipeg, Manitoba.

Brese, N.E., and O'Keeffe, M. (1991) Bond-valence parameters for solids. Acta Crystallographica, B47, 192–197.

Brown, I.D. (2013) http://www.iucr.org/__data/assets/file/0006/81087/bvparm2013.cif

Cooper, M.A., Hawthorne, F.C., and Grew, E.S. (2009) The crystal chemistry of the kornerupine-prismatine series. I. Crystal structure and site populations. Canadian Mineralogist, 47, 233–262.

Ercit, T.S., Anderson, A.J., Černý, P., and Hawthorne, F.C. (1986a) Bobfergusonite, a new phosphate mineral from Cross Lake, Manitoba. Canadian Mineralogist, 24, 599–604.

Ercit, T.S., Hawthorne, F.C., and Černý, P. (1986b) The crystal structure of bobfergusonite. Canadian Mineralogist, 24, 605–614.

Ercit, T.S., Tait, K., Cooper, M.A., Abdu, Y., Ball, N.A., Anderson, A.J., Černý, P., Hawthorne, F.C., and Galliski, M. (2010) Manitobaite, $Na_{16}Mn^{2+}_{25}Al_8(PO_4)_{30}$, a new phosphate mineral from Cross Lake, Manitoba, Canada. Canadian Mineralogist, 48, 1455–1463.

Hawthorne, F.C., Ungaretti, L., and Oberti, R. (1995) Site populations in minerals: terminology and presentation of results of crystal-structure refinement. Canadian Mineralogist, 33, 907–911.

Hughes, J.M., and Rakovan, J. (2002) The crystal structure of apatite, $Ca_5(PO_4)_3(F,OH,Cl)$. In M.L. Kohn, J. Rakovan, and J.M. Hughes, Eds., Phosphates: Geochemical, Geobiological and Materials Importance, p. 1–12. Reviews in Mineralogy and Geochemistry Vol. 48, Mineralogical Society of America, Chantilly, Virginia.

Hughes, J.M., Cameron, M., and Crowley, K.D. (1989) Structural variations in natural F, OH, and Cl apatites. American Mineralogist, 74, 870-876.

—— (1990) Crystal structures of natural ternary apatites: Solid solution in the $Ca_5(PO_4)_3X$ (X = F,OH,Cl) system. American Mineralogist, 75, 295–304.

Hughes, J.M., Ertl, A., Bernhardt, H.J., Rossman, G.R., and Rakovan, J. (2004) Mn-rich fluorapatite from Austria: crystal structure, chemical analysis and spectroscopic investigations. American Mineralogist, 89, 629–632.

Kreidler, E.R., and Hummel, F.A. (1970) The crystal chemistry of apatite: structure fields of fluor- and chlorapatite. American Mineralogist, 55, 170-184.

Lussier, A., Abdu, Y., Hawthorne, F.C., Michaelis, V.K., Aguiar, P.M., and Kroeker, S. (2011) Oscillatory zoned elbaite-liddicoatite from central Madagascar. I. Crystal chemistry and structure by SREF and ^{11}B and ^{27}Al MAS NMR spectroscopy. Canadian Mineralogist, 49, 63–88.

Mackie, P.E., Elliott, J.C., and Young, R.A. (1972) Monoclinic structure of synthetic $Ca_5(PO_4)_3Cl$, chlorapatite. Acta Crystallographica, B28, 1840-1848.

Pasero, M., Kampf, A.R., Ferraris, C., Pekov, I.V., Rakovan, J., and White, T.J. (2010) Nomenclature of the apatite supergroup minerals. European Journal of Mineralogy, 22, 163–179.

Pieczka, A. (2007) Beusite and an unusual Mn-rich apatite from the Szklary granitic pegmatite, Lower Silesia, Southwestern Poland. Canadian Mineralogist, 45, 901–914.

Pouchou, J.L., and Pichoir, F. (1985) 'PAP' φ(ρZ) procedure for improved quantitative microanalysis. In J.T. Armstrong, Ed., Microbeam Analysis, p. 104–106. San Francisco Press, California.

Shannon, R.D. (1976) Revised effective ionic radii and systematic studies of interatomic distances in halides and chalcogenides. Acta Crystallographica, A32, 751–767.

Sheldrick, G.M. (2008) A short history of SHELX. Acta Crystallographica, A64, 112–122.

Sudarsanan, K., Mackie, P.E., and Young, R.A. ((1972) Comparison of synthetic and mineral fluorapatite, $Ca_5(PO_4)_3F$, in crystallographic detail. Materials Research Bulletin, 1972, 1331-1338.

Suitch, P.R., Lacout, J.L., Hewat, A.W., and Young, R.A. (1985) The structural location and role of Mn^{2+} partially substituted for Ca^{2+} in fluorapatite. Acta Crystallographica, B41, 173–179.

Tait, K.T. (2002) The Crystal Chemistry of the Alluaudite-Group Minerals. MSc thesis, University of Manitoba, Winnipeg, Manitoba.

Tait, K.T., Ercit, T.S., Abdu, Y., Černý, P., and Hawthorne, F.C. (2011) The crystal structure and crystal chemistry of manitobaite, ideally $(Na_{16}\square)Mn^{2+}_{25}Al_8(PO_4)_{30}$, from Cross Lake, Manitoba. Canadian Mineralogist, 49, 1221–1242.

352 Yoder, C.N., Fedors, N., Flora, N.J., Brown, H., Hamilton, K., and Schaeffer, C.D. Jr. (2004)
353 The existence of pure-phase transition metal hydroxy apatites. Synthesis and Reactivity
354 in Inorganic and Metal-Organic Chemistry, 34, 1835-1842.
355

FIGURE CAPTIONS

Figure 1. The (a) Raman and (b) infrared spectra of pieczkaite.

Figure 2. Comparison of the stereochemistry around the M1 site in (a) hydroxylapatite, (b) fluorapatite, (c) chlorapatite, (d) pieczkaite; Ca: yellow circles; Mn: violet circles; O: blue circles; the numbers inside the circles indicate the specific anion identifications given in the original papers.

Figure 3. Comparison of the stereochemistry around the M2 site in (a) hydroxylapatite, (b) fluorapatite, (c) chlorapatite, (d) pieczkaite; legend as in Fig. 2, plus orange circles represent monovalent anions. All monovalent-anions sites except that of F half-occupied (i.e., disordered off special positions on the 6_3 axis) ; both sites are shown but only one is locally occupied.

Figure 4. Comparison of the stereochemistry around the monovalent-anion site in (a) hydroxylapatite, (b) fluorapatite, (c) chlorapatite, (d) pieczkaite; legend as in Fig. 2, plus orange circles represent monovalent anions.

TABLE 1. Chemical composition (wt%) of pieczkaite

Constituent	wt%	Range	SD
P_2O_5	37.52	35.28-39.51	0.83
MnO	41.77	19.64-47.46	6.51
FeO	2.45	1.07-3.35	0.56
CaO	13.78	7.02-33.81	6.22
Cl	3.86	2.88-4.19	0.37
H_2O	0.60		
O = Cl	-0.87		
Total	99.11		

TABLE 2. Powder-diffraction data for pieczkaite

$I_{(meas.)}$ %	$d_{(meas.)}$ Å	$d_{(calc.)}$ Å	h	k	l	$I_{(meas.)}$ %	$d_{(meas.)}$ Å	$d_{(calc.)}$ Å	h	k	l
8	8.231	8.231	0	1	0	17	1.810	1.810	-3	5	1
5	5.026	5.026	0	1	1			1.810	-2	5	1
4	4.116	4.115	0	2	0	16	1.796	1.796	-4	5	0
15	3.453	3.453	0	2	1			1.796	-1	5	0
24	3.174	3.174	0	0	2	**22**	1.750	1.749	-2	3	3
14	3.111	3.111	-2	3	0			1.749	-1	3	3
		3.111	-1	3	0	14	1.727	1.728	-1	5	1
12	2.961	2.961	0	1	2			1.726	0	4	2
100	2.794	2.793	-2	3	1	10	1.623	1.623	-3	5	2
		2.793	-1	3	1	12	1.587	1.586	0	0	4
88	2.744	2.744	0	3	0			1.584	-3	6	0
34	2.639	2.639	-1	2	2	3	1.563	1.563	-4	5	2
25	2.514	2.518	0	3	1			1.563	-1	5	2
		2.513	0	2	2	7	1.555	1.556	-4	6	0
11	2.283	2.283	-3	4	0			1.556	-2	6	0
		2.283	-1	4	0			1.556	-3	4	3
11	2.224	2.225	-2	4	1			1.552	-1	4	3
		2.222	-2	3	2	3	1.537	1.537	-3	6	1
		2.222	-1	3	2	5	1.511	1.511	-4	6	1
9	2.148	2.148	-3	4	1			1.511	-2	6	1
		2.148	-1	4	1	2	1.478	1.480	0	2	4
6	1.933	1.933	-1	2	3			1.478	-5	6	0
21	1.902	1.902	-2	4	2			1.478	-1	6	0
10	1.889	1.888	-3	5	0			1.475	0	4	3
		1.888	-2	5	0	9	1.461	1.461	0	5	2
25	1.853	1.853	-3	4	2	7	1.440	1.440	-5	6	1
		1.853	-1	4	2			1.440	-1	6	1

TABLE 3. Miscellaneous refinement data for pieczkaite

a (Å)	9.504(4)
c	6.347(3)
V (Å^3)	496.5(1)
Space group	$P6_3/m$
Z	2
D_{calc} (g/cm^3)	3.783
Radiation/ filter	Mo*K*α
2θ-range for data collection (°)	50.00
R(int) (%)	1.96
Reflections collected	42095
Reflections in Ewald sphere	12637
Independent reflections $F_o > 4\sigma F$	2292 2288
Refinement method	Full-matrix least squares on F^2
$R_{(merge)}$ %	1.96
Final R_{obs} (%) [$F^o > 4\sigma F$]	R_1 = 4.06
R indices (all data) (%)	R_1 = 2.22 wR_2 = 5.99 GooF = 1.126

$R_1 = \Sigma(|F_o| - |F_c|) / \Sigma|F_o|$

$wR_2 = [\Sigma w(F_o^2 - F_o^2)^2 / \Sigma(F_o^2)^2]^2$, $w = 1/[\sigma^2(F_o)^2 + (0.0279\ P)^2 + (14.20\ P)]$, where $P = (Max(F_o^2,0) + 2\ F_o^2) / 3$

Table 4. Atom coordinates and displacement parameters for pieczkaite

Site	*x*	*y*	*z*	U_{11}	U_{22}	U_{33}	U_{23}	U_{13}	U_{12}	U_{eq}
M1	⅓	⅔	-0.0060(3)	0.0092(8)	0.0092(8)	0.0203(12)	0	0	0.0046(4)	0.0129(7)
M2	0.7291(2)	0.7532(2)	¼	0.030(6)	0.0186(10)	0.0227(10)	0	0	0.0148(8)	0.0225(7)
P	0.5955(3)	0.9725(3)	¼	0.0090(12)	0.0066(12)	0.0267(14)	0	0	0.0034(10)	0.0143(8)
X	0	0	0.2179(13)	0.021(2)						
O(1)	0.6486(8)	0.1527(8)	¼	0.018(3)	0.007(3)	0.027(4)	0	0	0.003(3)	0.0186(16)
O(2)	0.4081(8)	0.8675(8)	¼	0.006(3)	0.009(3)	0.050(5)	0	0	0.002(3)	0.0226(18)
O(3)	0.6565(6)	0.9219(6)	0.0564(9)	0.029(3)	0.021(3)	0.029(3)	-0.001(2)	0.001(2)	0.018(2)	0.0243(13)

TABLE 5. Selected interatomic distances (Å) in pieczkaite

M1-O1a,b,c	2.254(5)	M2-O2e	2.233(7)
M1-O2,d,e	2.331(5)	M2-O3f,g	2.163(6)
M1-O3	2.833(5)	M2-O3,h	2.379(5)
		M2-Xi	2.477(2)
P-O1f	1.525(7)		
P-O2	1.547(7)		
P-O3,g	1.535(5)		
<P-O>	1.536		

a: *y*, -*x*+*y*+1, *z*; b: -*x*+1, -*y*+1,-*z*; c: *x*-*y*, *x*, -*z*; d: -*y*+1, *x*-*y*+1, *z*; e: -*x*+*y*, -*x*+1, *z*; f: *x*-*y*+1, *x*, -*z*; g: *x*-*y*+1, *x*, *z*+½; h: *x*, *y*, -*z*+½; i: *x*+1, *y*+1, *z*; j: *x*+1, *y*+1, -*z*+½.

TABLE 6. Refined site-scattering values and site populations for pieczkaite

Site	Site scattering (epfu)	Site population (apfu)	Mean bondlength (Å)
M1	45.8(6)	1.15 Mn* + 0.85 Ca	2.293
M2	72.3(9)	2.46* Mn + 0.54 Ca	2.324
X	15.9(4)	0.72 Cl + 0.28 (OH)	

* includes 0.26 Fe.

TABLE 7. Bond valences (v.u.) for pieczkaite*

	M1	M2	*P*	Σ
O1	0.359 $^{x3\downarrow\ x2\rightarrow}$		1.282	2.000
O2	0.292 $^{x3\downarrow\ x2\rightarrow}$	0.335	1.208	2.127
O3	[0.075 $^{x3\downarrow}$]	0.405 $^{x2\downarrow}$ 0.226 $^{x2\downarrow}$	1.248 $^{x2\downarrow}$	1.879 [1.954]
X		**0.377 $^{x3\rightarrow}$		1.131
Σ	1.953 [2.151]	1.974	4.986	

*calculated with the parameters of Brown (2013) and Brese and O'Keeffe (1991);

** the X-site is half occupied and hence contributes x1 summed around M2.

TABLE 8. Comparison of selected interatomic distances (Å) in some apatite-supergroup structures

	$Ca_3(PO_4)_3(OH)$	$Ca_3(PO_4)_3F$	Pieczkaite	$Ca_3(PO_4)_3Cl$					
M1-O1 x3	2.404	2.392	2.254	Ca1	2.426, 2.371, 2.447	Ca2	2.387, 2.398, 2.438		
M1-O2 x3	2.451	2.451	2.331	Ca1	2.416, 2.395, 2.478	Ca2	2.498, 2.438, 2.412		
M1-O3 x3	2.802	2.810	2.833	Ca1	2.942, 2.851, 2.654	Ca2	2.942, 2.729, 2.664		
<M1-O>	2.552	2.551	2.473	Ca1	2.553	Ca2	2.545		
M2-O1	2.710	2.818	3.161	Ca3	2.965	Ca4	2.973	Ca5	2.972
M2-O2	2.353	2.384	2.233	Ca3	2.296	Ca4	2.300	Ca5	2.299
M2-O3 x2	2.343	2.395	2.163	Ca3	2.314, 2.361	Ca4	2.357, 2.323	Ca5	2.321, 2.351
M2-O3 x2	2.509	2.383	2.380	Ca3	2.470, 2.609	Ca4	2.556, 2.507	Ca5	2.459, 2.620
M2-X	2.385 x2	2.229 x2	2.477 x2	Ca3	2.789, 3.236	Ca4	2.813, 3.218	Ca5	2.800, 3.234

TABLE 9. Interatomic distances and corresponding bond-valences

	X-Ca (Å)	Bond valence (v.u.)	Bond-valence sum (v.u.)
$Ca_3(PO_4)_3F$	2.229	0.351	1.05
$Ca_3(PO_4)_3(OH)$	2.385	0.323	0.97
$Ca_3(PO_4)_3Cl$	2.801	0.312	0.94
Pieczkaite	2.477	0.340	1.02

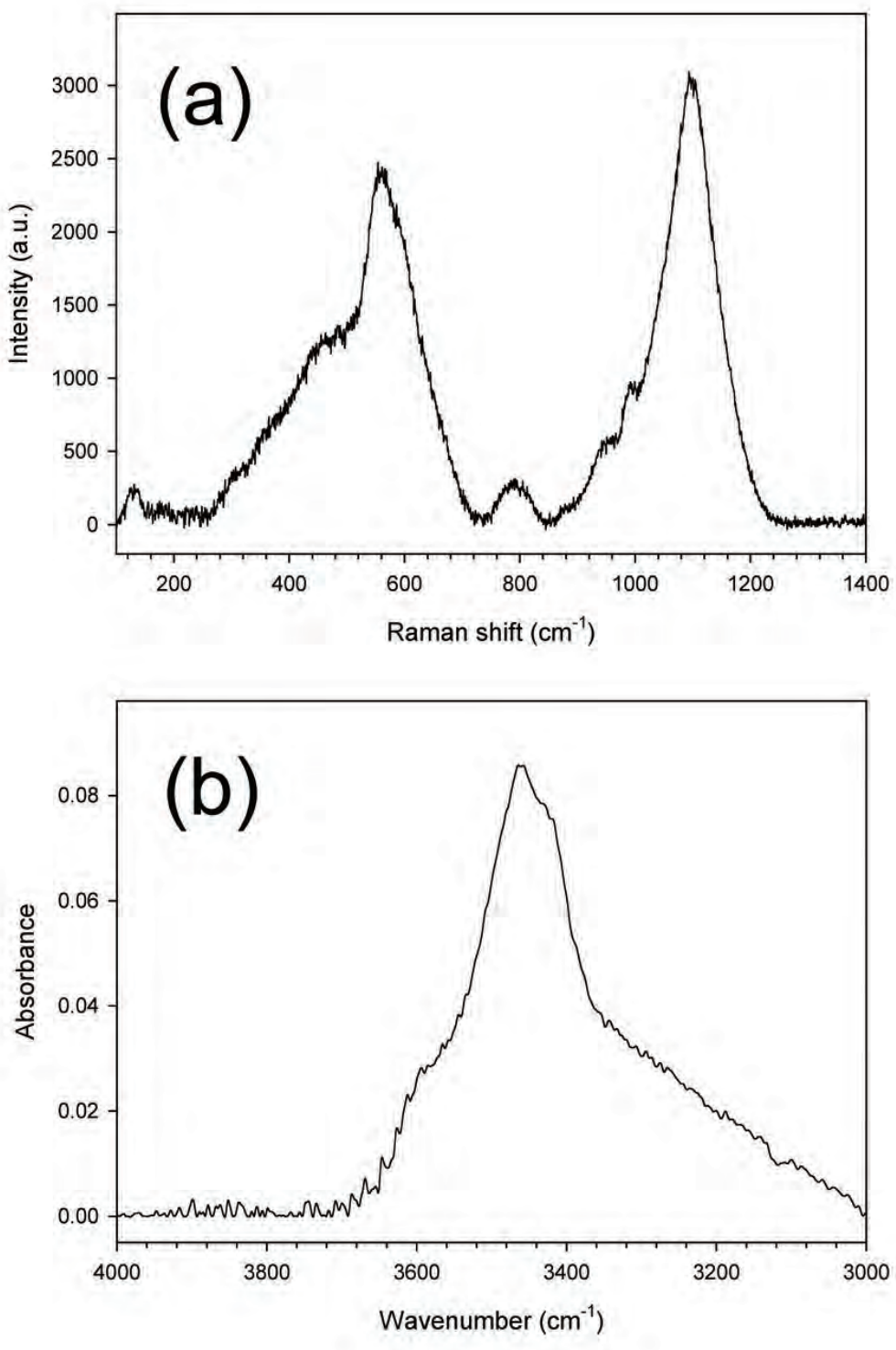
(a)
Intensity (a.u.)
0
500
1000
1500
2000
2500
3000
200
400
600
800
1000
1200
1400
Raman shift (cm-1)
(b)
Absorbance
0.00
0.02
0.04
0.06
0.08
4000
3800
3600
3400
3200
3000
Wavenumber (cm-1)

FIGURE 1

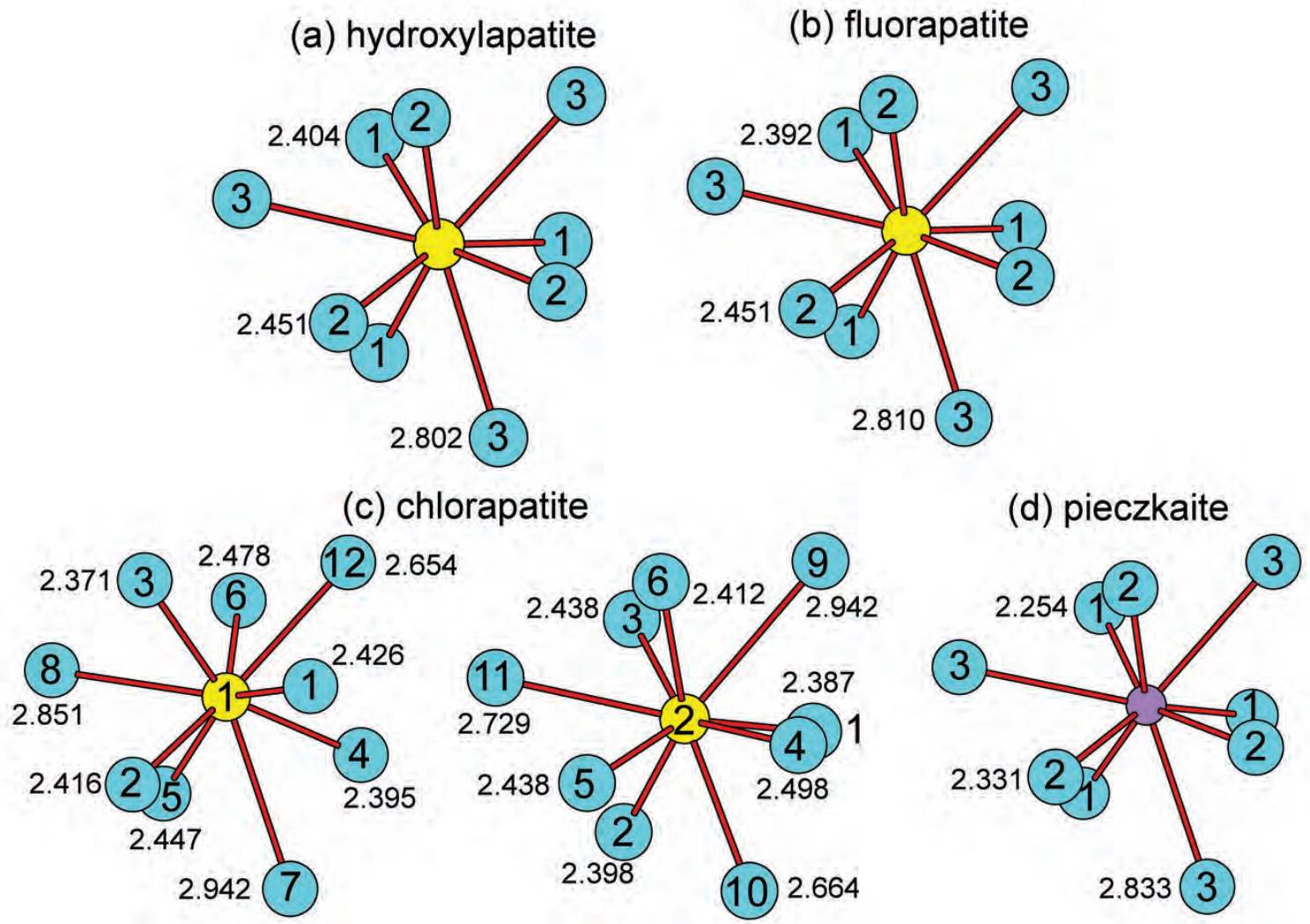
(a) hydroxylapatite
2.404
2.451
2.802
(b) fluorapatite
2.392
2.451
2.810
(c) chlorapatite
2.371
2.478
2.654
2.426
2.851
2.416
2.447
2.395
2.942
2.438
2.412
2.942
2.387
2.729
2.438
2.498
2.398
2.664
(d) pieczkaite
2.254
2.331
2.833

FIGURE 2

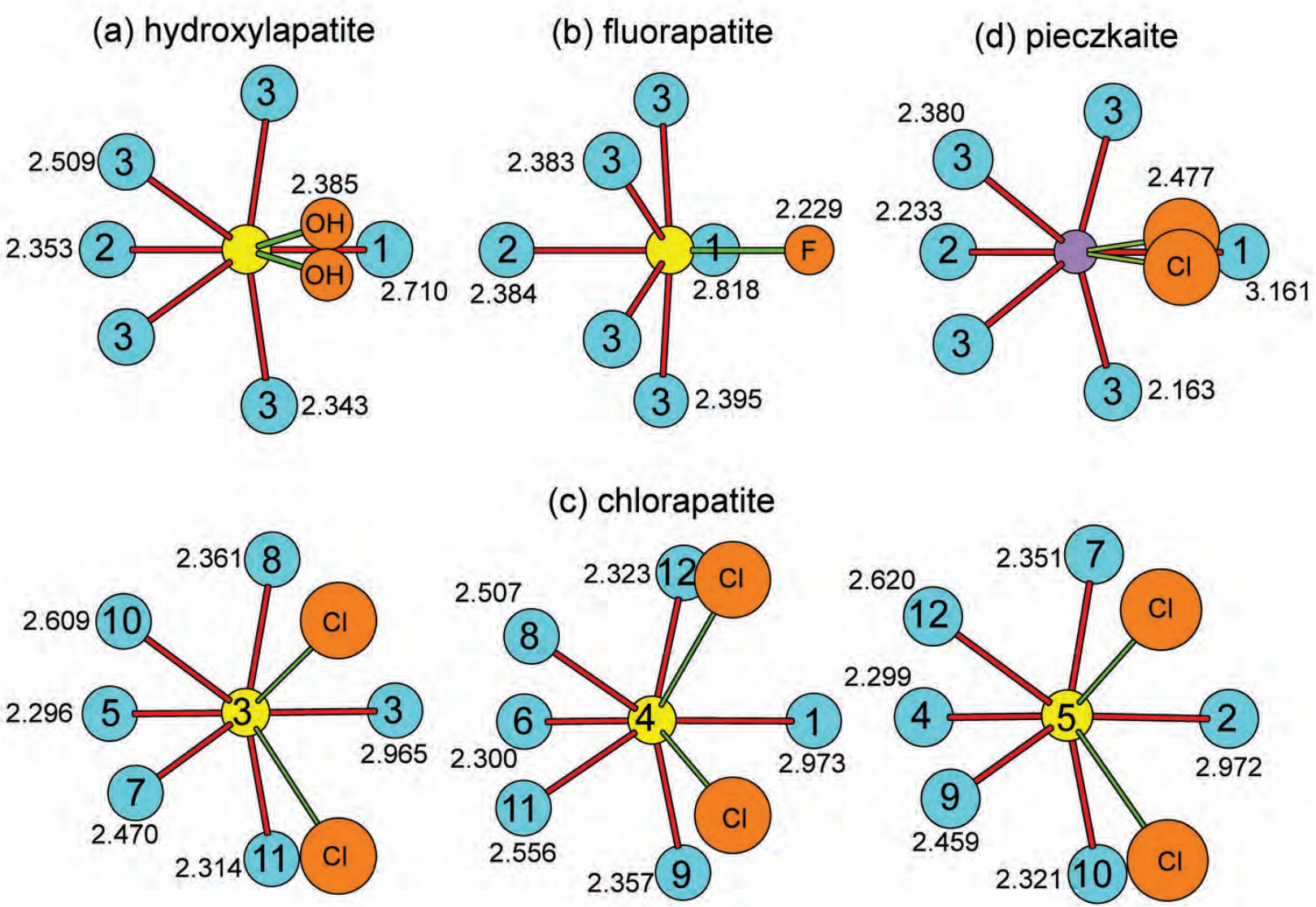
(a) hydroxylapatite
3
2.509
3
2.385
OH
2.353
2
1
OH
2.710
3
3
2.343
(b) fluorapatite
3
2.383
3
2.229
2
1
F
2.384
2.818
3
3
2.395
(d) pieczkaite
2.380
3
3
2.477
2.233
2
Cl
1
3.161
3
3
2.163
(c) chlorapatite
2.361
8
Cl
2.609
10
2.296
5
3
3
2.965
7
2.470
2.314
11
Cl
2.507
2.323
12
Cl
8
6
4
1
2.300
2.973
11
Cl
2.556
2.357
9
2.351
7
2.620
Cl
12
2.299
4
5
2
2.972
9
2.459
2.321
10
Cl

FIGURE 3

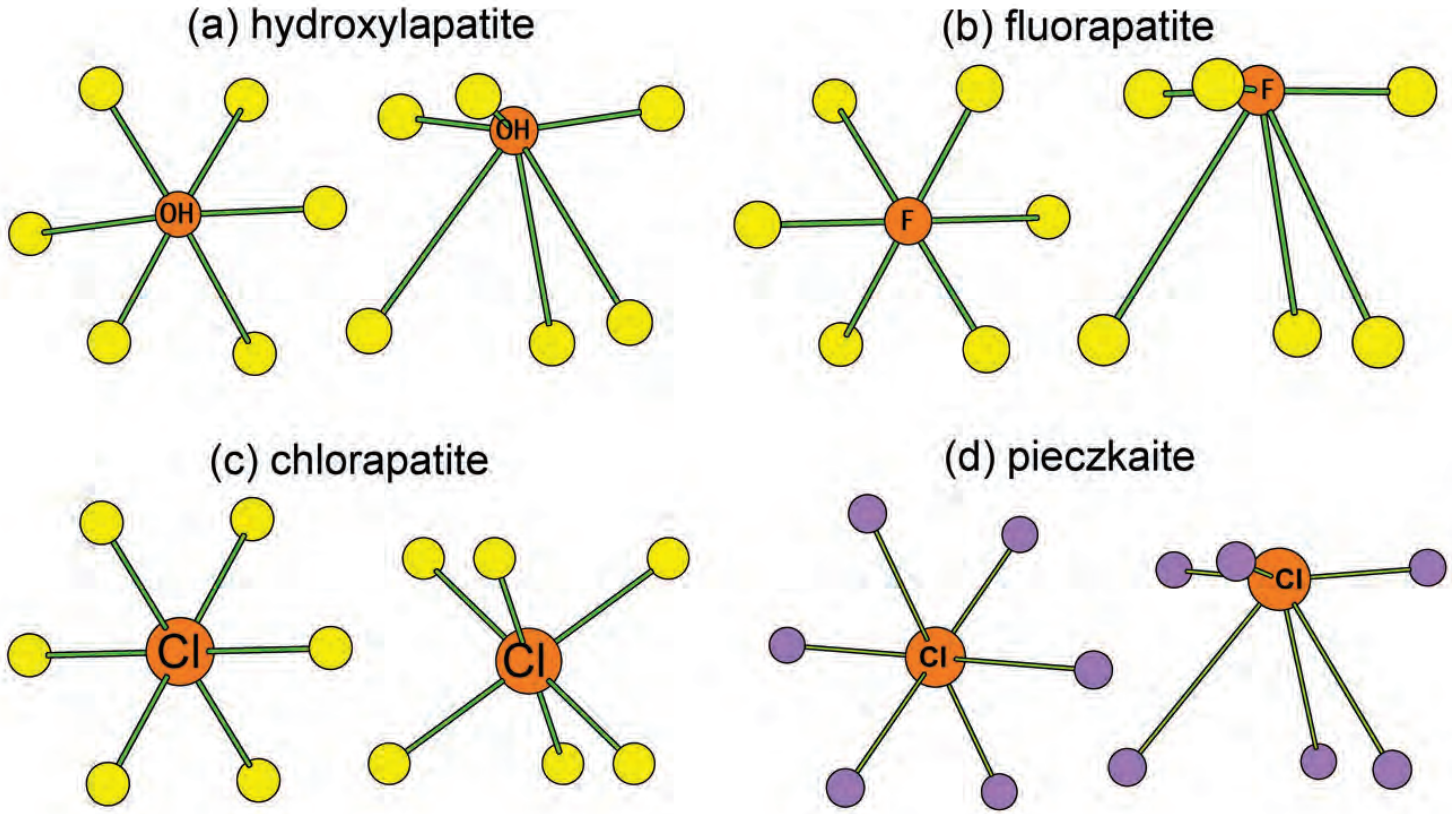
(a) hydroxylapatite
OH
OH
(b) fluorapatite
F
F
(c) chlorapatite
Cl
Cl
(d) pieczkaite
Cl
Cl

FIGURE 4